

## Comparison of Photocatalytic Activity and Cyclic Voltammetry of Zinc Oxide and Titanium Dioxide Nanoparticles toward Degradation of Methylene Blue

S.O. Fatin.<sup>1</sup>, H.N. Lim<sup>2,\*</sup>, W.T. Tan<sup>2</sup>, N.M. Huang<sup>1</sup>

<sup>1</sup> Low Dimensional Materials Research Centre, Department of Physics, Faculty of Science, University of Malaya, 50603 Kuala Lumpur, Malaysia.

<sup>2</sup> Department of Chemistry, Faculty of Science, Universiti Putra Malaysia, 43400 UPM Serdang, Selangor, Malaysia.

\*E-mail: [janet\\_limhn@science.upm.edu.my](mailto:janet_limhn@science.upm.edu.my)

Received: 15 July 2012 / Accepted: 31 August 2012 / Published: 1 October 2012

---

We report on the photocatalytic degradation of methylene blue (MB) solution using commercial ZnO and TiO<sub>2</sub> (P25) photocatalysts, in the form of slurry and immobilized on glass slides, under ultraviolet (UV) and solar irradiations. The average particle sizes of ZnO and P25 were 100 nm and 30 nm, respectively. Under both the irradiations, the photocatalytic activities of ZnO and P25 slurry resulted in better photocatalytic performance than the immobilized photocatalysts. Interestingly, ZnO showed better degradation capability in comparison to P25 under the solar irradiation. This result revealed that solar light provided a good source of energy to degrade MB in the presence of ZnO. The cyclic voltammetry analysis suggested that the photocatalysts possessed different mechanisms for the degradation of MB. The potential of immobilizing photocatalysts without compromising their performance may lead to easy handling of these materials, resulting in expanding their applications, for example, as a photoanode for photoelectrochemistry.

---

**Keywords:** ZnO; TiO<sub>2</sub>; solar; thin film

### 1. INTRODUCTION

The removal of organic pollutants in waste water using semiconductor photocatalysts has attracted a lot of attention as an important issue on environmental protection [1-5]. Photocatalytic oxidation is an economical process owing to the fact that it involves only a photocatalyst and light source [6]. This process does not yield toxic intermediate product, making it suitable for cleaning water environment that contains low to medium contaminants concentration [7]. Under the

illumination of light that have energies higher than the photocatalyst band gap, the electrons from the valence band will be excited to the conduction band, therefore, creating the negative electron-positive hole pairs ( $e^- - h^+$ ). The  $e^- - h^+$  pairs will initiate a series of reactions and produce hydroxyl radicals,  $HO^\bullet$ , and superoxide radical anions,  $O^{\bullet-2-}$ , when the photocatalyst is in contact with water. With the radicals on the photocatalyst surface, the organic contaminants are oxidized at or near to the photocatalyst surface [8].

Titanium dioxide, particularly P25, is found to be the most efficient photocatalyst for photodegradation of pollutants due to its properties which are suitable band gap (3.2 eV), photo stable and nontoxic [9]. Besides  $TiO_2$ , zinc oxide (ZnO) has also shown promise as an innovative and relatively low-cost photocatalyst. ZnO is an n-type semiconductor that possesses suitable band gap (3.17 eV), large exciton binding energy (60 meV) and high electron mobility [10].

Photocatalysis requires the mixing of the powder photocatalyst into the pollutant water, resulting in slurry suspension of photocatalyst. It is almost impossible to obtain powder-free water after the photocatalysis process, making it an impractical solution to getting pristine water [11]. This problem limits its practical application, following the need of centrifugation and consumes time for settlement. Therefore, many attempts have been made to immobilize the catalyst particles on a rigid support by different approaches [12]. Even though immobilized photocatalyst has lower efficiency when compared with photocatalyst in the slurry form because of the smaller interface surface available, the disadvantage is outweighed by the practicality of reusing immobilized photocatalyst, which makes it suitable to be applied for continuous water treatment. Hence, long-term attachment of photocatalyst on the support must be guaranteed so that it can be reused in the next treatment [13].

Many researchers reported using UV irradiation as an energy source in the photocatalytic degradation of organic compounds [14-16]. The drawbacks of UV light are that it is hazardous, may affect the photocatalyst decomposition and expensive because of large input of electric power to generate radiation [17]. Solar light consists of only 5% of the total radiation that possesses the optimum energy for the band gap excitation of electrons; however, in tropical countries like Malaysia where intense sunlight is abundant and available throughout the year, it is a safe and cost-effective source.

In this paper, the photocatalytic behavior of P25 was compared against ZnO in the forms of slurry and immobilized on a glass slide under the illumination of UV and solar lights for the degradation of MB solution, which is reported for the first time. Moreover, this is the first ever attempt in which cyclic voltammetry analysis is used to determine the degradation mechanism of photocatalysts. This fundamental and preliminary work is important to gauge if the performance of immobilized photocatalyst would be compromised compared to that of the slurry form. Moreover, this work is able to assess if the solar energy is comparable to UV for the photocatalysis process. This work could lead to more investigations on photoelectrochemistry, in which immobilized photocatalyst on indium tin oxide (ITO) coated glass acts as a photoanode.

## 2. EXPERIMENTAL

### 2.1. Materials

Zinc oxide was purchased from Aldrich (99%, St. Louis, USA), titanium (IV) oxide Aeroxide P25 was purchased from Acros Organics (99.5%, New Jersey, USA), methylene blue was purchased from System (Selangor, Malaysia) and all the solutions were prepared using distilled water.

### 2.2. Preparation of immobilized photocatalysts

ZnO slurry was prepared by mixing ZnO powder with distilled water. The ZnO slurry was then smeared onto a glass slide using the doctor blade's method to produce immobilized ZnO. The dimension of the coating on the glass slide for the solar and UV irradiation test was fixed at 4 cm × 2 cm with a mass of 12 mg. Then, the coating was calcined at 450 °C for 2 h. The adherence of the photocatalyst on the glass slide was tested by immersing the film in stirred water for 3 days, in which no flotation was observed. Immobilized P25 was prepared using the same procedure. The same amount of photocatalyst, used for immobilization, was calcined independently at 450 °C for 2 h, which was subsequently employed in the form of slurry for photocatalytic evaluation.

### 2.3. Characterization

Crystalline phase was determined using a PanAnalytical Empyrean X-Ray Diffractometer (XRD), employing a scanning rate of 0.12 °C/min in a 2θ range from 20° to 70° with Cu Kα radiation ( $\lambda = 1.5418 \text{ \AA}$ ). The morphologies of ZnO and TiO<sub>2</sub> photocatalysts were obtained using a FEI Nova NanoSEM 400 Field Emission Scanning Electron Microscope (FESEM). The change in the photodegradation of the MB solution was determined using an Ultraviolet-Visible Spectrophotometer Evolution 300 (UV-Vis) by measuring its absorbance spectra within 500 nm to 750 nm.

### 2.4. Photocatalytic activity

The photocatalytic activities were evaluated by decolorization of 1.5 ppm of MB solution. For UV irradiation, the immobilized photocatalyst was placed inside a beaker containing 100 ml of MB solution. Then, the beaker was placed inside an Ultraviolet Crosslinker (UVP-CL-1000, Cambridge) with 5800  $\mu\text{W}/\text{cm}^2$  intensity which was stacked onto a magnetic stirrer. The beaker was exposed under the UV irradiation for 30 m with a stirring rate of 200 rpm. The distance between the photocatalyst and the light source was fixed at 13 cm. In the case of slurry photocatalyst, the MB solution was separated from the photocatalyst by centrifugation at 4000 rpm. The experiment was repeated for solar irradiation using a solar simulator Oriel Instrument (AM 1.5; Newport Corporation, Irvine, CA, USA) with 8220  $\mu\text{W}/\text{cm}^2$  intensity from 150 W Xe lamp. Both the irradiations were repeated without the presence of photocatalysts in the MB solution.

### 2.5. Cyclic Voltammetry

Cyclic voltammetry (CV) study was performed on a VersaSTAT 3 potentiostat (Ametek Princeton Applied Research, Oak Ridge, TN) using a conventional three-electrode system. The working electrode was a photocatalyst powder-modified glassy carbon electrode (GCE) (3 mm diameter, Princeton Applied Research), the reference electrode was an Ag/AgCl (in 3M NaCl) electrode, and the counter electrode was a platinum wire. The GCE was polished successively using 0.1  $\mu\text{M}$  of alumina slurry on a micro-cloth polishing pad (Buehler, Lake Bluff, IL), and rinsed thoroughly with distilled water between each polishing step. For preparation of photocatalyst-modified GCE, the bare GCE was tapped onto the photocatalyst powder. The electrochemical response of 1.5 ppm of MB solution was investigated in 0.1 M of KCl supporting electrolyte by cyclic scanning between -1.0 V and 1.0 V at a scan rate  $50 \text{ mVs}^{-1}$ . All the voltammetric measurements were carried out at room temperature. The photoactivity of ZnO and P25 against the MB solution was measured by exposing the reactant to solar light from the solar simulator for 2 h. The data was recorded every 20 min.

### 3. RESULT AND DISCUSSION

The structural characterization and electron microscopy observation of the photocatalysts are to ensure that their crystallinities and morphologies remained the same after being subjected to the heat treatment for their immobilization on glass slides. Fig. 1a shows that the ZnO powder can be well indexed to the hexagonal wurtzite structure [18]. The absence of other impurity peaks indicates the clear crystallinity of the ZnO powder. Meanwhile, Fig. 1b shows the XRD patterns of P25 having peaks indicative of the reflections for anatase and rutile with no other peaks of impurity [19]. The final forms of the photocatalysts experienced insignificant differences when exposed to the heat treatment, suggesting that ZnO and  $\text{TiO}_2$  are stable enough to retain their characteristic structures despite the harsh condition.

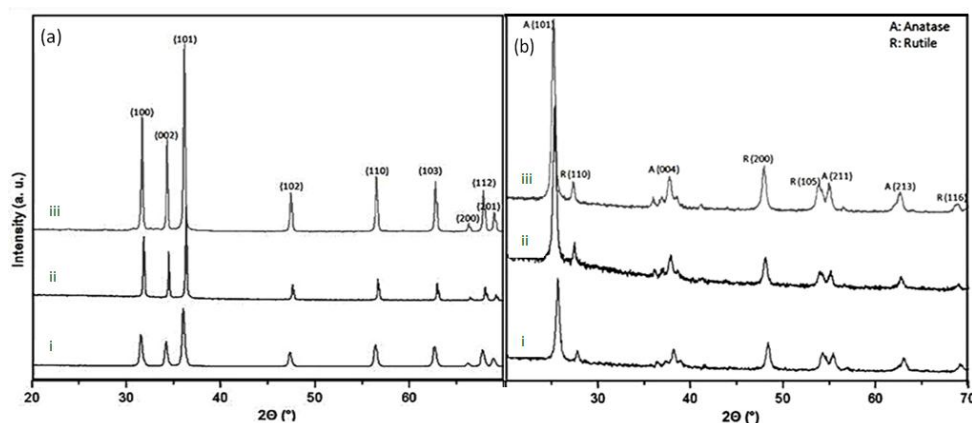


**Figure 1.** XRD patterns of (ai) calcined ZnO, (aai) ZnO film, (aiii) ZnO pure powder, (bi) calcine P25, (bii)  $\text{TiO}_2$  film, and (biii)  $\text{TiO}_2$  pure powder.

Fig. 2 shows the SEM images of the nanostructures of ZnO and P25. The morphologies of both ZnO and P25 remained unchanged after calcination regardless of whether they were in the powder form or immobilized on glass slides. The size of ZnO is 100 nm, which is about three times larger than that of P25.

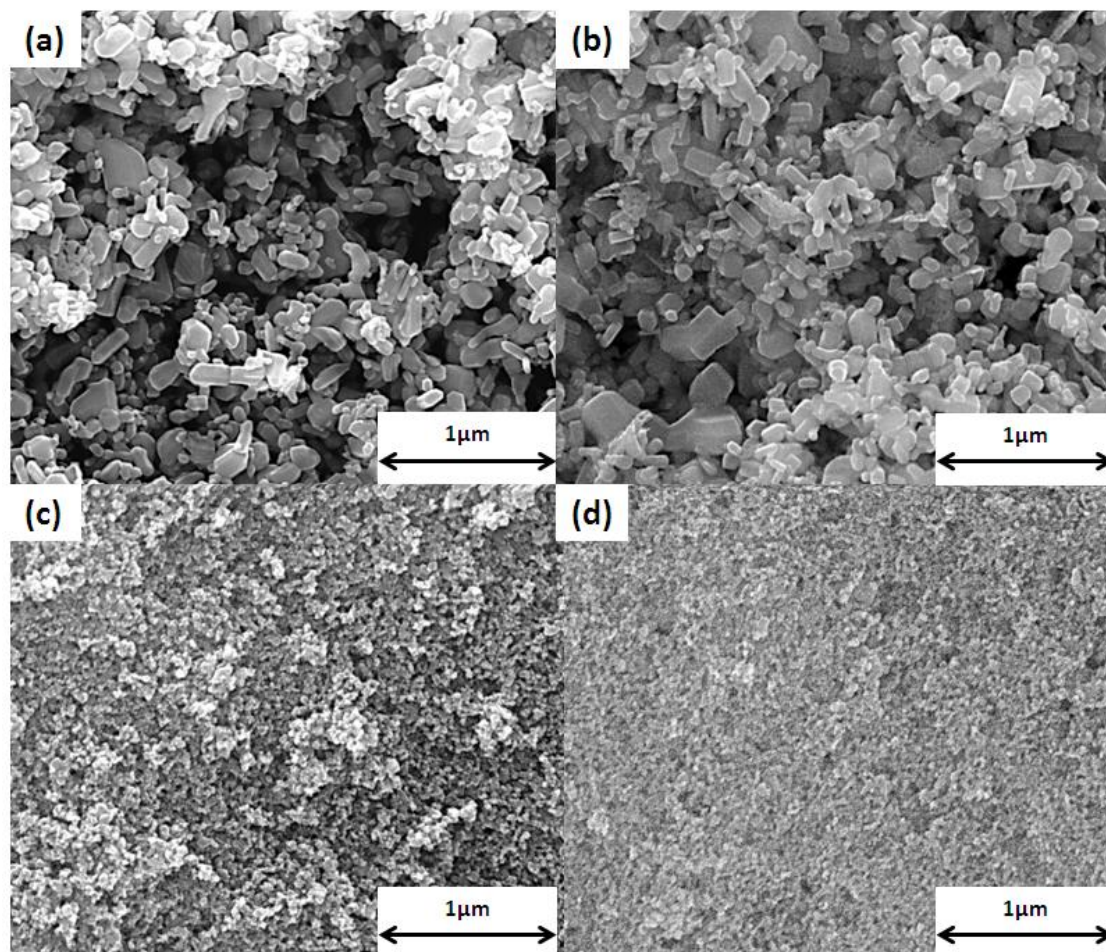


**Figure 2.** SEM images of (a) ZnO powder after calcination, (b) immobilized ZnO after calcinations, (c) P25 powder after calcination, and (d) immobilized P25 after calcination.

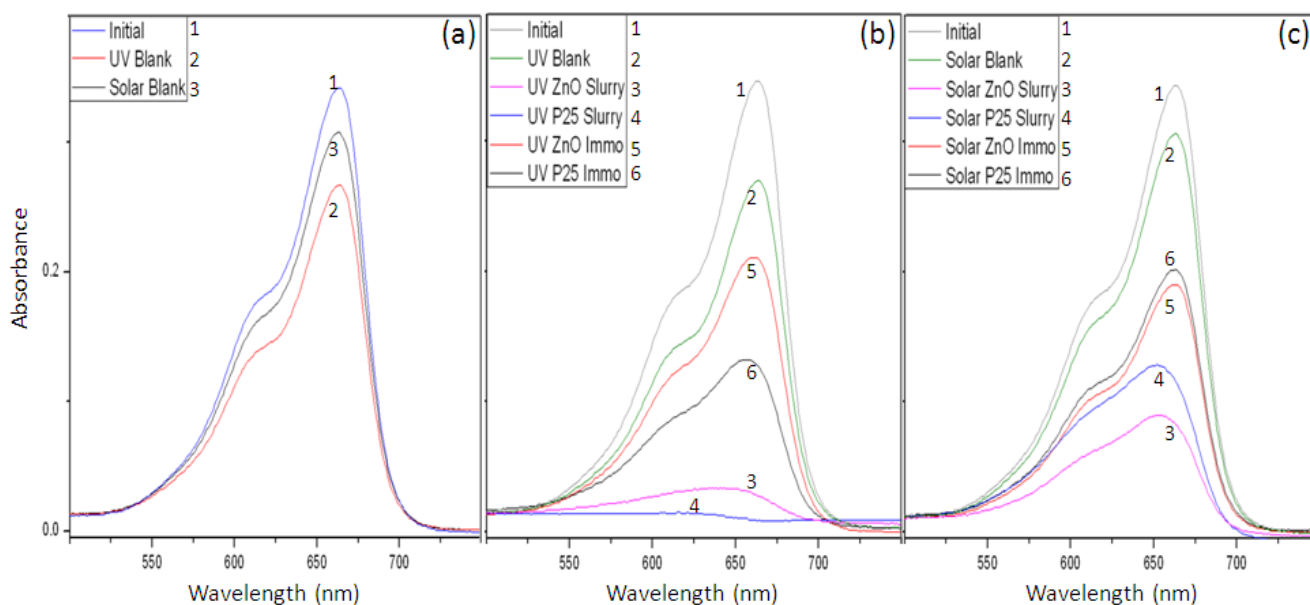
Fig. 3 exhibits that the absorbance spectra of the MB solution have a maximum absorption wavelength at approximately 660 nm. Fig. 3a portrays the absorbance spectra of the MB photodegradation in the absence of photocatalyst. After 30 min of illumination, the peak under the UV and solar irradiations reduced compared with the initial concentration. This is due to photolytic reaction of MB induced by the absorption of UV light and solar light, which leads to the degradation of MB [20]. The peak for UV irradiation is lower than the peak for solar irradiation, showing that the photon energy of UV irradiation is higher than that of solar irradiation.

Fig. 3b exhibits the absorbance spectra of the MB degradation under the UV irradiation. The ZnO and P25 slurries were found to be more efficient in photocatalyzing the MB solution compared with the immobilized counterparts. The peaks of the MB solution with P25 are lower than those of

ZnO, both in the slurry and immobilized forms. The enhanced photocatalytic performance of P25 is contributed by its ability to strongly absorb UV rays due to its high band gap energy [21, 22]. It has been reported that the photodegradation capability of ZnO is weaker than P25 under the illumination of UV light [23].

Fig. 3c portrays the absorbance spectra of MB degradation under the solar light irradiation. Similarly, the slurries of ZnO and P25 were found to be better in degrading the MB solution than the immobilized ZnO and P25. In contrast to the irradiation by UV light, the photocatalytic activity of ZnO outperformed that of P25, both in the slurry or immobilized forms. Some studies have confirmed that ZnO exhibits better efficiency than  $\text{TiO}_2$  in photocatalytic degradation of some dyes when sunlight is used as an energy source because ZnO is able to absorb a large fraction of solar spectrum than  $\text{TiO}_2$  [24, 25]. Meanwhile,  $\text{TiO}_2$  can only absorb the UV fraction of the solar light, which attributes to only 2-5% of the solar spectrum [26, 27].

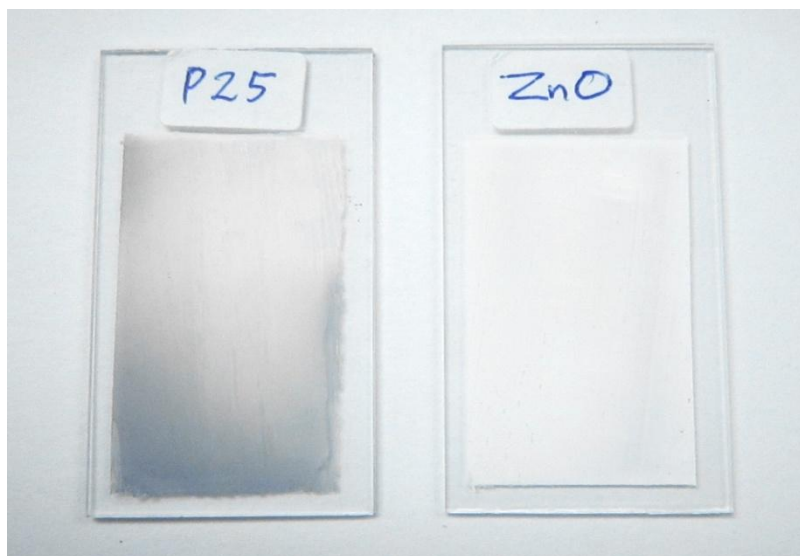
Under both the UV and solar irradiations, the immobilized photocatalysts show lower activities compared to the slurry photocatalysts due to the decrease in the interfacial area between the MB solution and the photocatalyst [28]. The mass of ZnO and P25 on the glass slides was unaltered before and after the reaction, suggesting that the photocatalysts were not leached from the substrate during the reaction.



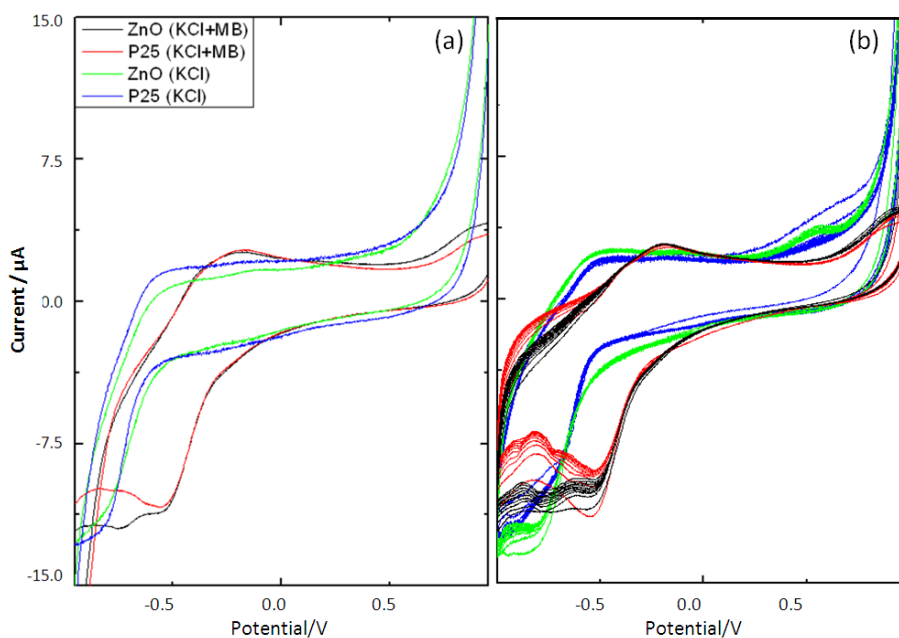
**Figure 3.** UV-Vis absorption spectra of the MB solution (a) without photocatalyst, (b) with photocatalyst under UV light, and (c) with photocatalyst under solar light.

Fig. 4 shows the appearance of the immobilized photocatalysts after the degradation of MB solution. The immobilized P25 was tainted blue but the immobilized ZnO remained white. This is an indication that the degradation mechanism of P25 differs to that of ZnO. Therefore, we investigated the degradation mechanism of both the photocatalysts through cyclic voltammetric (CV) analysis under

the irradiation of solar light. Solar ray is the preferred source of light because it is renewable, sustainable, inexpensive and abundant compared to UV ray.



**Figure 4.** Photoimage of immobilized P25 and ZnO film after the photocatalysis process



**Figure 5.** (a) CV and (b) multiple CV of modified GCE in 0.1 M of KCl solution with and without the presence of 1.5 ppm of MB.

In Fig. 5a, the background current behavior for the GCE modified with photocatalyst in KCl supporting electrolyte exhibits non-existence of peak. On the contrary, in the presence of MB in KCl supporting electrolyte, two peaks appeared at -0.25 V on the oxidation scan and -0.5 V on the

reduction scan. Fig. 5b shows that the current associated with oxidation and reduction shifted slightly after the tenth potential cycle for the photocatalyst-modified GCE. The presence of MB has little influence on the oxidation and reduction peaks as they remained at almost the same intensity. Moreover, the peaks are well-defined and remain unaltered during the cycles, reflecting the stability of photocatalyst coating on the GCE [29, 30].

Fig. 6 shows the CV for unmodified and modified GCE in the dark for 2 h. The curves stayed the same, indicating that the degradation of MB solution did not occur when the photocatalysts were not exposed to solar light.

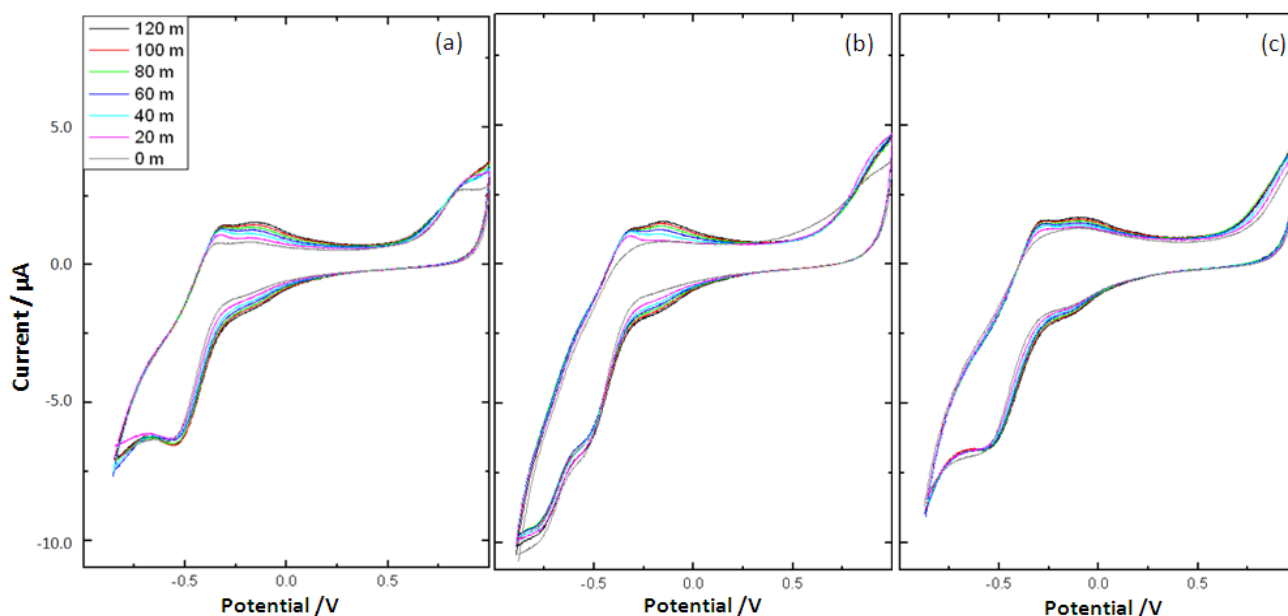


**Figure 6.** CV for (a) bare GCE, (b) ZnO-modified GCE, and (c) P25-modified GCE in 0.1 M of KCl solution spiked with 1.5 ppm of MB left in the dark for 2 h.

On the other hand, the CV patterns of the photocatalysts changed upon the illumination with solar light for 2 h, as portrayed in Fig. 7. When the GCE was not modified with any photocatalyst, there is hardly any enhancement or decrement in the cycles after 2 h (Fig. 7a), signifying inefficient redox process of MB in the absence of photocatalyst. On the contrary, upon modification with the photocatalysts, there is an obvious shift in the cycles, suggesting that the electrochemical response of the photocatalysts toward MB happened significantly when the reaction was exposed to the solar light. In fact, ZnO and P25 present different direction in the shift. The difference is because of the adsorptive behavior of the MB on the photocatalyst [31]. Based on Fig. 7b, the anodic peak current increased but cathodic peak current decreased with increasing scan number, which may be contributed by the gradual degradation of MB molecules by ZnO [32, 33]. While in Fig. 7c, both the redox peak currents are significantly enhanced with increasing scan cycle, indicating that the MB layer was adsorbed on the surface of P25 for each cycle [34, 35, 36]. These findings are in agreement with the photoimage shown in Fig. 4 where the P25 film was covered with a layer of blue color after the photodegradation

reaction whereas the ZnO film was untainted. The CV result shows that the degradation mechanism for ZnO occurred directly where the MB molecules were immediately mineralized upon contact with ZnO, as opposed to P25 in which adsorption is important in the degradation process.

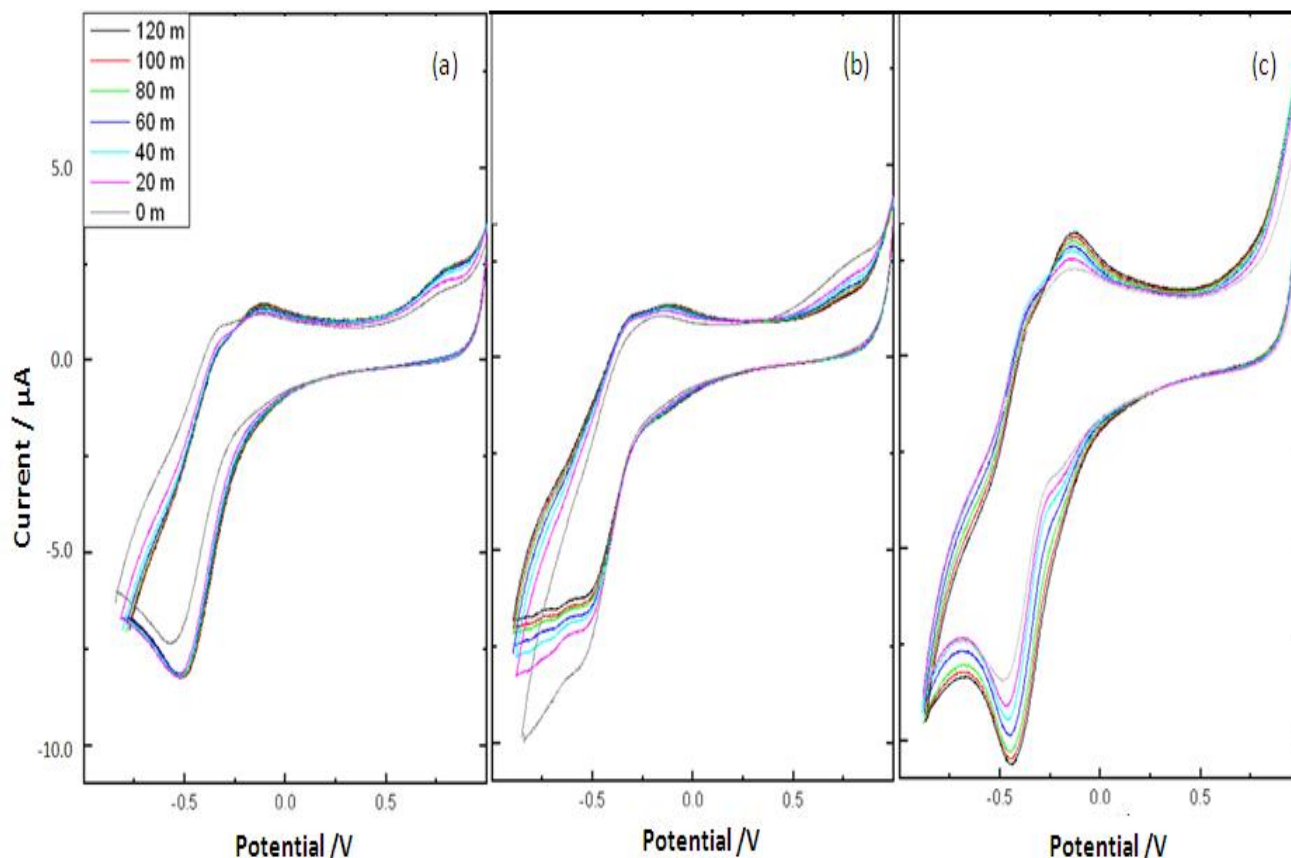


**Figure 7.** CV for (a) bare GCE, (b) ZnO-modified GCE, and (c) P25-modified GCE in 0.1 M of KCl solution spiked with 1.5 ppm of MB illuminated with solar light for 2 h.

#### 4. CONCLUSION

From the results obtained, nanostructured ZnO and P25 photocatalysts presented excellent photodegradation of MB under the UV and solar irradiations. ZnO provides an effective and suitable alternative to P25 for the degradation of MB solution under the illumination of solar light. The CV analysis showed that MB adsorbed on the surface of P25 before the onset of degradation, whereas ZnO degraded MB immediately upon contact with the molecules. The photocatalysts had proven to be still effective even after adherence on the glass substrate, which in turn promises to be an option for a more extensive solar application such as using it as a photoanode for photoelectrochemistry water-splitting hydrogen evolution.

## ACKNOWLEDGEMENT

This work was supported by Loreal Malaysia 'For Women in Science Fellowships' 2011, the High Impact Research Grant of the University of Malaya (UM.C/625/1/HIR/030) and the High Impact Research Grant from the Ministry of Higher Education (UM.C/625/1/HIR/MOHE/05).

## References

1. Y. Wang, Y. He, T. Li, J. Cai, M. Luo and L. Zhao, *Catal. Commun.*, 18 (2012) 161-164.
2. M.N. Rashed and A.A. El-Amin, *Int. J. Phys. Sci.*, 2 (2007) 073-081.
3. W.S. Chiu, P.S. Khiew, M. Cloke, D. Isa, T.K. Tan, S. Radiman, R. Abd-Shukor, M.A. Abd. Hamid, N.M. Huang, H.N. Lim and C.H. Chia, *Chem. Eng. J.*, 158 (2010) 345-352.
4. N.S. Anwar, A. Kassim, H.N. Lim, S.A. Zakarya and N.M. Huang, *Sains Malaysiana*, 39 (2010) 261-265.
5. S.A. Zakarya, A. Kassim, H.N. Lim, N.S. Anwar and N.M. Huang, *Sains Malaysiana*, 39 (2010) 975-979.
6. J. Ru, Z. Huayue, L. Xiaodong and X. Ling, *Chem. Eng. J.*, 152 (2009) 537-542.
7. J. Studnickova and T.A. Mofokeng, 7th International Conference, 6-8 Sep. 2010, Liberec, Czech Republic (World Journal of Engineering, China, 2010) 119.
8. M. Soltaninezhad and A. Aminifar, *Int. J. Nano Dimension*, 2 (2011) 137-145.
9. D. Wang, J. Zhang, Q. Luo, X. Li, Y. Duan and J. An, *J. Hazard. Mater.*, 169 (2009) 546-550.
10. J. Huang, C. Xia, L. Cao and X. Zeng, *Mater. Sci. Eng. B*, 150 (2008) 187-193.
11. M.H. Habibi and A. Elham, *Iran. J. Catal.*, 1 (2011) 41-44.
12. A.H. Amar, MSc thesis, Universiti Sains Malaysia (Penang, Malaysia, 2007).
13. R.V. Grieken, J. Marugán, C. Sordo and C. Pablos, *Catal. Today*, 144 (2009) 48-54.
14. C.K. Sheng, W.M.M. Yunus, W.M.Z.W. Yunus, Z.A. Talib and M.M. Moxsin, *Solid State Sci. Tech.*, 11 (2003) 124-130.
15. C.M. Ling, A.R. Mohamed and S. Bhatia, *Jurnal Teknologi*, 40(F) (2004) 91-103.
16. S.K. Kavitha and P.N. Palanisamy, *Mod. Appl.*, 4 (2010) 5.
17. B. Neppolian, H.C. Choi, S. Sakthivel, B. Arabindoo and V. Murugesan, *J. Hazard. Mater B*, 89 (2001) 303-317.
18. Y. Dai, Y. Zhang, Q.K. Li and C.W. Nan, *Chem. Phys. Lett.*, 358 (2002) 83-86.
19. X.T. Zhou, H.B. Ji and X.J. Huang, *Mol.*, 17 (2012) 1149-1158.
20. J. Tschirch, R. Dillert, D. Bahnemann, B. Proft, A. Biedermann and B. Goer, *Res. Chem. Intermed.*, 34 (2008) 381-392.
21. J. Shen, Y. Zhu, X. Yang and C. Li, *J. Mater. Chem*, 22 (2012) 13341-13347.
22. M. Janczarek, J. Hupka and H. Kisch, *Physicochem. Prob. Miner. Process.*, 40 (2006) 287-292.
23. G.Y.M.A. Nour, MSc thesis, An-Najah National University (Nablus, Palestine, 2009).
24. K. Yogendra, S. Naik, K.M. Mahadevan and N. Madhusudhana, *Int. J. Environ. Sci. Res.*, 1, (2011) 11-15.
25. S. Sakthivel, B. Neppolian, M.V. Shankar, B. Arabindoo, M. Palanichamy and V. Murugesan, *Sol. Energy Mater. Sol. Cells*, 77 (2003) 65-82.
26. M. Janczarek, H. Kisch and J. Hupka, *Physicochem. Prob. Miner. Process.*, 41 (2007) 159-166.
27. K. Hashimoto, H. Irie and A. Fujishima, *Jpn. J. Appl. Phys.*, 44 (2005) 8269-8285.
28. R.C. Meena, R.B. Pachwarya, V.K. Meena and S. Arya, *Am. J. Environ. Sci.*, 5 (2009) 444-450.
29. H.N. Lim, R. Nurzulaikha, I. Harrison, S.S. Lim, W.T. Tan and M.C. Yeo, *Int. J. Electrochem. Sci.*, 6 (2011) 4329-4340.
30. W.Y. Liu and K.J. Zhang, *Int. J. Electrochem. Sci.*, 6 (2011) 1066 - 1074.
31. C.X. Ruana, J. Lou, Y.Y. Duan and W. Sun, *J. Chin. Chem. Soc.*, 57 (2010) 1056-1060.

32. N.H. Rahman, T.W. Tee and K. Sirat, *Int. J. Electrochem. Sci.*, 6 (2011) 3118-3128.
33. A.M. Zaky, S.S.A.E. Rehim and B.M. Mohamed, *Int. J. Electrochem. Sci.*, 1 (2006) 17-31.
34. J.J. Huang, W.S. Hwang, Y.C. Weng and T.C. Chou, *Mater. Trans.*, 51 (2010) 2294 – 2303.
35. C.X. Xu, K.J. Huang, Y. Fan, Z.W. Wu and J. Li, *J. Mol. Liq.*, 165 (2012) 32-37.
36. Sh. Abbasi, M. Allahyari, Z. Taherimaslak, D. Nematollahi and F. Abbasi, *Int. J. Electrochem. Sci.*, 4 (2009) 602 – 613.